Percolation cluster statistics of 2D Lennard-Jones phases

1989 J. Phys.: Condens. Matter 1 6217

(http://iopscience.iop.org/0953-8984/1/35/020)

J. Phys.: Condens. Matter 1 (1989) 6217–6230. Printed in the UK

Percolation cluster statistics of 2D Lennard-Jones phases

N Cooper†, A Tedder†, D M Heyes†‡ and John R Melrose§
† Department of Chemistry, Royal Holloway and Bedford New College, University of London, Egham, Surrey TW20 0EX, UK
§ Department of Physics, Imperial College, University of London, London SW7 2BZ, UK

Received 12 December 1988, in final form 17 April 1989

Abstract. The percolation cluster characteristics of 2D Lennard-Jones (LJ) fluid and solid phases have been determined by molecular dynamics computer simulation. The variation of the percolation threshold with temperature from the soft-core to hard-core limits is reported and interpreted in terms of changes in the short-range structure. The distribution of clusters is analysed using the cluster number distribution function, n_s. Based in the small systems considered, we find that at the percolation threshold, the measured percolation exponent τ departs from the universal 2D value of 2.05, ranging from 1.6 ± 0.1 in the soft-core limit to 2.0 ± 0.05 in the hard-core limit. However, the fractal dimension of the clusters, D_f, at the percolation threshold is indistinguishable from the 2D universal value of 1.9, having the range 1.9 ± 0.1 for all state points considered. The same trends are observed in 3D LJ fluids. We examine the time dependence of the percolating clusters and show them to be ephemeral on a molecular timescale.

1. Introduction

Percolation studies have until recently been confined to non-interacting occupied sites randomly placed on a lattice. The importance of percolation in many physical sciences has prompted studies of interacting particles on lattice sites and in continuum space (Balberg and Binenbaum 1987). In this report we continue our investigation into the percolation cluster statistics of *interacting* continuum ('off-lattice') systems explored using molecular dynamics (MD) computer simulation. In the previous report (Heyes and Melrose 1988), the percolation cluster statistics of the 3D Lennard-Jones (LJ) fluid were described. Here we investigate the corresponding 2D fluid. We consider the effect of temperature and cluster definition (through the assumed connectivity distance) on the percolation threshold and statistics. A new feature of this work is that we examine the time dependence of the percolating clusters.

2. Cluster and percolation theory

Our method of determining clusters is identical to that used previously (Heyes and Melrose 1988, 1989). The operational definition for particles belonging to the same cluster is that each member is separated from *at least* one of the others by a distance $\leqslant \sigma_s$.

‡ Author to whom all correspondence should be addressed.

0953-8984/89/356217 + 14 $02.50

The disk of diameter σ_s around each LJ particle is called a soft-shell. As σ_s diminishes, the repulsive core of the particle exerts a greater influence on the nature of the clusters formed out of the soft-shells since it restricts the extent of overlap of the shells. This we term the soft-core to hard-core transition.

We evaluated the function, P, the fraction of configurations (time steps) generated by the computer that manifested at least one percolating cluster (PC). The percolation threshold in the thermodynamic limit (i.e., $N \to \infty$) p_c is best estimated for finite N when $P = 0.5$, because it shows the smallest system size (i.e., N) dependence.

The distribution of different sized clusters is characterised by the cluster number distribution function, n_s, which for these continuum systems is the time-average number of clusters containing s particles, N_s divided by N, i.e., $n_s = N_s/N$ (Balberg 1988). For finite periodic systems there is an upper bound on s, i.e., $1 \leqslant s \leqslant N$, resulting in distortions for $s \to N$. At the percolation threshold (Stauffer 1984).

$$n_s(p_c) \propto s^{-\tau}. \tag{1}$$

At the percolation threshold, the radius of gyration R_g provides a route to the fractal dimension D_f of the non-percolating clusters (Herrmann 1986)

$$R_g = \tfrac{1}{2}\left\langle \sum_{i}^{s-1} \sum_{j \neq i}^{s} R_{ij}^2/s(s-1) \right\rangle^{1/2}. \tag{2}$$

where R_{ij} is the vector separation between particles i and j. The scaling relationship here is $R_g \propto s^{1/D_f}$ as $s \to \infty$.

The pair radial distribution function $g(r)$ and pair connectedness function $p(r)$ for pair separations r are probes of the local structure in the whole fluid and in the percolating clusters, respectively (Seaton and Glandt 1987)

$$g(r) = n(r)/(2\pi r \rho \delta r). \tag{3}$$

where δr is the radial increment for $n(r)$; $n(r)$ is the number of particles found on average within $r - \delta r/2 \leqslant r \leqslant r + \delta r/2$.

If P_∞ is the fraction of molecules in the percolating cluster PC then

$$p(r) = n(r)' P_\infty/(2\pi r \rho \delta r). \tag{4}$$

where $n(r)'$ is the number of particles found on average within $r - \delta r/2 \leqslant r \leqslant r + \delta r/2$ within the PC. The search for pairs in $p(r)$ is restricted to those particles within the same PC, As $r \to \infty$ then $p(r) \to P_\infty^2$. For finite r there is a regime in which $p(r) \sim r^{D_f - 2}$. For the small N considered here it is hardly possible to go out far enough in r to determine D_f *in the hard-core limit* because the density oscillation from the short-range structure obscures the small decrease in $p(r)$ with r at short separations. The $p(r)$ look similar to the $g(r)$ but attain a lower limiting value. When the pair separation becomes comparable to the size of the periodic cell, the dimension of the PC must approach the dimension of the space, D (= 2 here).

3. Simulation details

The details of the MD technique used for particles interacting via the LJ potential

$$\phi(r) = 4\varepsilon[(\sigma/r)^{12} - (\sigma/r)^6], \tag{5}$$

have been described elsewhere (Heyes 1987). The MD simulations were performed on

square unit cells of area A containing $N = 50$, 450 and 1250 particles. The Verlet algorithm was used to increment the positions of the molecules. We use LJ reduced units throughout, i.e., $k_B T/\varepsilon \rightarrow T$, and number density, $p = N\sigma^2/A$. Equilibrium simulations were made, during which the density was adjusted to locate the percolation threshold. These extended for 16 reduced time units for $N = 450$. These were followed by a production simulation of 8 reduced time units to accumulate the reported quantities.

4. Results and discussion

In figure 1 the boundary lines between percolating and non-percolating states are presented superposed on the 2D LJ phase diagram (e.g. Reddy and O'Shea 1985). Percolation occurs to the right of each line. A range of σ_s is considered, which spans essentially the entire LJ phase diagram. Despite increasing statistical uncertainty in the soft-core limit, the results are consistent with the limit $\phi_s = \pi p \sigma_s^2/4\sigma^2 \rightarrow 0.94$, observed by Bug *et al* (1985) for square-well fluids. The figure reveals very much the same trend as for the 3D fluid (Heyes and Melrose 1988). The main features of the 2D fluids are:

(i) In the hard-core limit (e.g., $\sigma_s \leqslant 1.15$), in the ordered 'solid' phase, the value of p_c increases with decrease in temperature from $T = 10 \rightarrow 0.6$, the range considered here.

(ii) The $\sigma_s = 1.2$ and 1.5 lines manifest a curvature to lower density as T decreases from $T = 2$ to $T = 0.6$.

(iii) The $\sigma_s \geqslant 2.0$ lines vary less with temperature between $T = 2.0$ and $T = 0.6$. The low temperature curvature is small but towards higher density. The effect becomes less pronounced for $\sigma_s \geqslant 3.0$.

These different regimes of behaviour result from changes in short-range structure. The regimes (ii) and (iii) follow the same pattern as the square-well fluids of Bug *et al*

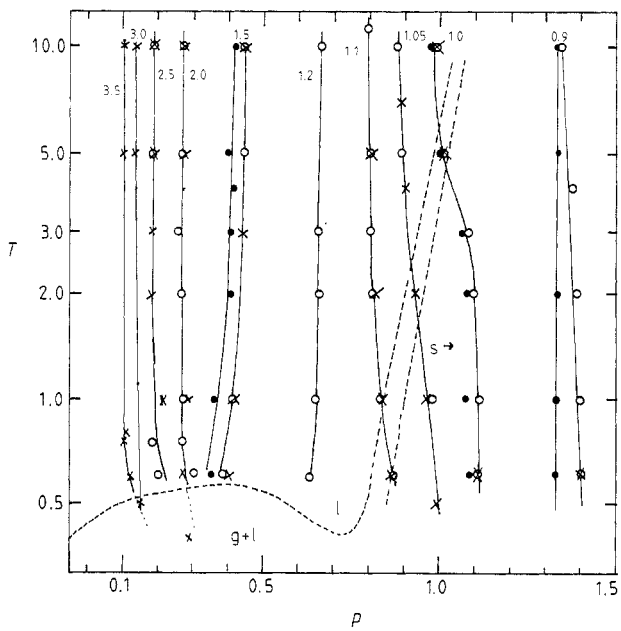

Figure 1. The percolation thresholds for the 2D LJ solid and fluid superposed on its phase diagram. The full curves denote boundaries between non-percolating states (to the left) and percolating states (to the right) of the curves. Distance is in LJ σ. Each line corresponds to and is annotated by a particular search diameter σ_s in LJ units. ●, $N = 50$; ○, $N = 450$; ×, $N = 1250$. The broken curves mark the phase boundaries between gas (g), liquid (l) and solid (s). LJ reduced units are used as defined in § 3.

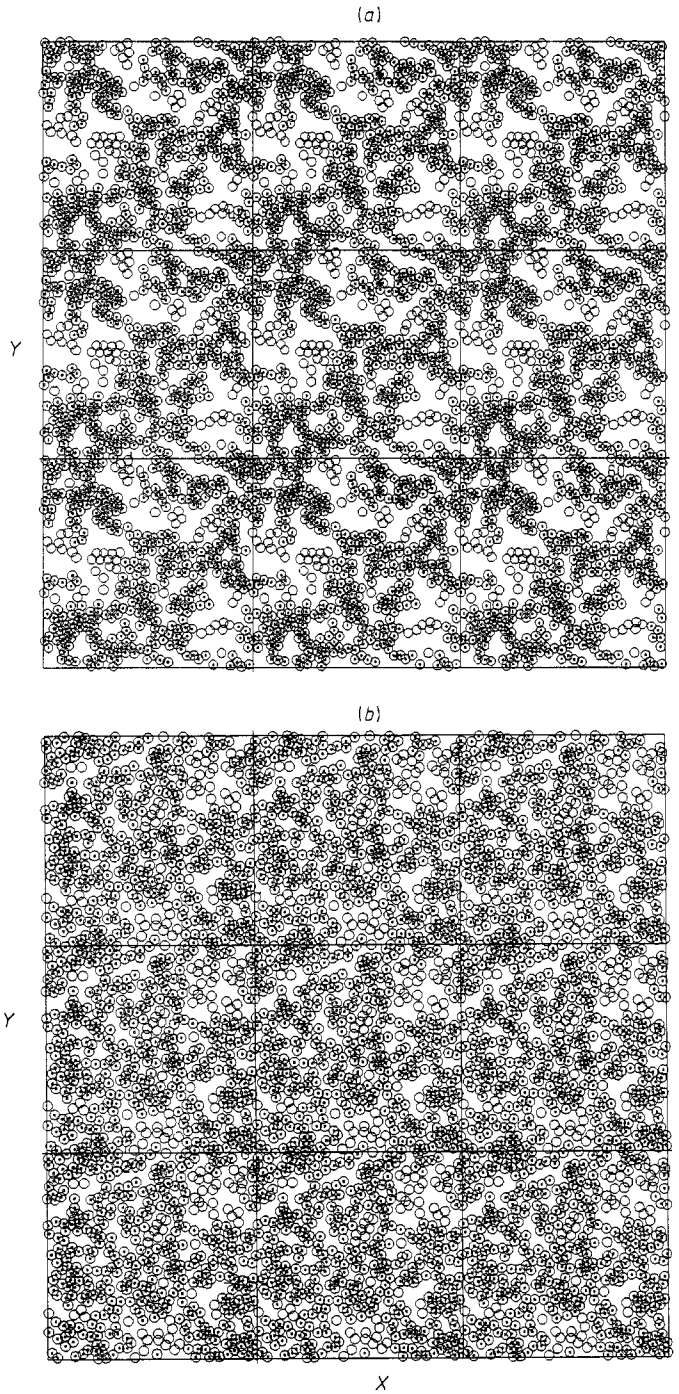

Figure 2. Pictorial illustration of non-percolating and percolating clusters in two-dimensional periodically repeating cells at the percolation threshold, taken from 2D LJ MD simulations with $\sigma_s = 1.5$. The outer dashed circles are the soft cores of the LJ molecules (of diameter σ_s). The central square is the real MD cell; the surrounding cells are its images. The cluster with ⊙ is percolating. The clusters with ○ are non-percolating. (*a*) $p_c = 0.388$, $T = 0.6$; (*b*) $p_c = 0.441$, $T = 10.0$; $N = 450$.

(1985). In case (ii), as $T \rightarrow T_c$, (the critical temperature) the percolating clusters being more tenuous. The 'branches' of the PC are thinner and held together more tightly with the drop in temperature to T_c. This is illustrated in figure 2. The percolation threshold density correspondingly *decreases*. This is caused by an enhanced local connectivity as temperature drops, without causing a severe contraction in the number of nearest neighbours within σ_s. Figure 3 presents pair-radial, $g(r)$, distribution functions and r-dependent coordination numbers, $n_c(r)$, illustrating this point. The first two peaks in $g(r)$ become larger as the temperature drops, even though at $r = 1.15$ the coordination number is statistically the same for $T = 1.0$ and $T = 10.0$.

Further into the soft-core regime a drop in temperature causes greater bunching of the soft-shells on the $\sim\sigma_s$ distance scale. These regions are joined by short thinner 'strings' of particles, sometimes called 'necks'. We have made the transition from a 'stringy' percolating cluster to another form of PC consisting of 'blobs' of soft-shells connected by narrow 'node-links'. Consequently, the percolation threshold *increases*. This is seen clearly in the instantaneous configurations presented in figure 4. The $g(r)$ and $n_c(r)$ in figure 5 demonstrates the growth of the first co-ordination shell and enhancement of coordination number at σ_s, which makes percolation less likely as temperature decreases. Higher densities are therefore required to achieve $p \rightarrow p_c$.

Although, regimes (i) and (iii) manifest similar p_c temperature dependences, the microscopic origins are different. In regime (i) the particles pack in a triangular lattice, evident in figure 6. As the temperature drops the first peak in $g(r)$ moves to higher r, revealed in figure 7. As $\sigma_s \leqslant \sigma$ here, this shift moves many neighbours outside the soft-shell range. Therefore the density needs to increase to induce percolation. In this regime the PC consists of broad bands of particles at all temperatures. The non-percolating cluster 'holes' are bigger at lower temperature.

Percolation below $p_c(N)$ (i.e., when $P = 0.5$) is purely a finite-N artefact. As the density decreases below p_c the percolating cluster decreases dimensionality below D_f at p_c. This is because the PC condition is satisfied with the aid of the periodic boundary conditions. It is statistically more probable for the PC to form along the cell axes than along any other direction because fewer particles are required to connect across the simulation cell and hence over all space. In figure 8 we show this behaviour for $\varepsilon = (p_c - p)/p = 0.005$ and 0.1 for $T = 10$ and $\sigma_s = 1.2$, where $p_c = 0.662$.

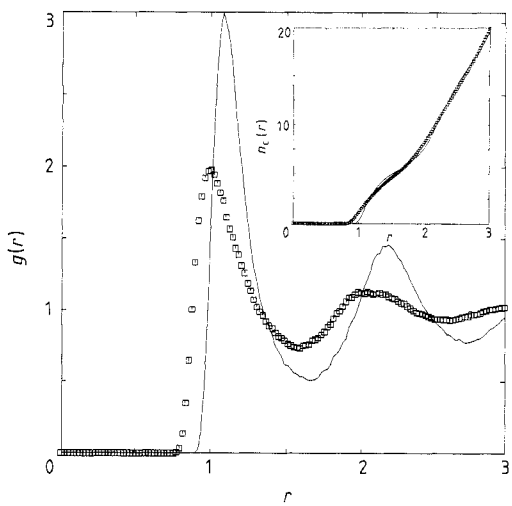

Figure 3. The pair radial distribution function $g(r)$ for $N = 50$ states at $p = 0.75$. The full curve corresponds to $T = 1.0$ and □ correspond to $T = 10.0$. Inset: the derived coordination numbers.

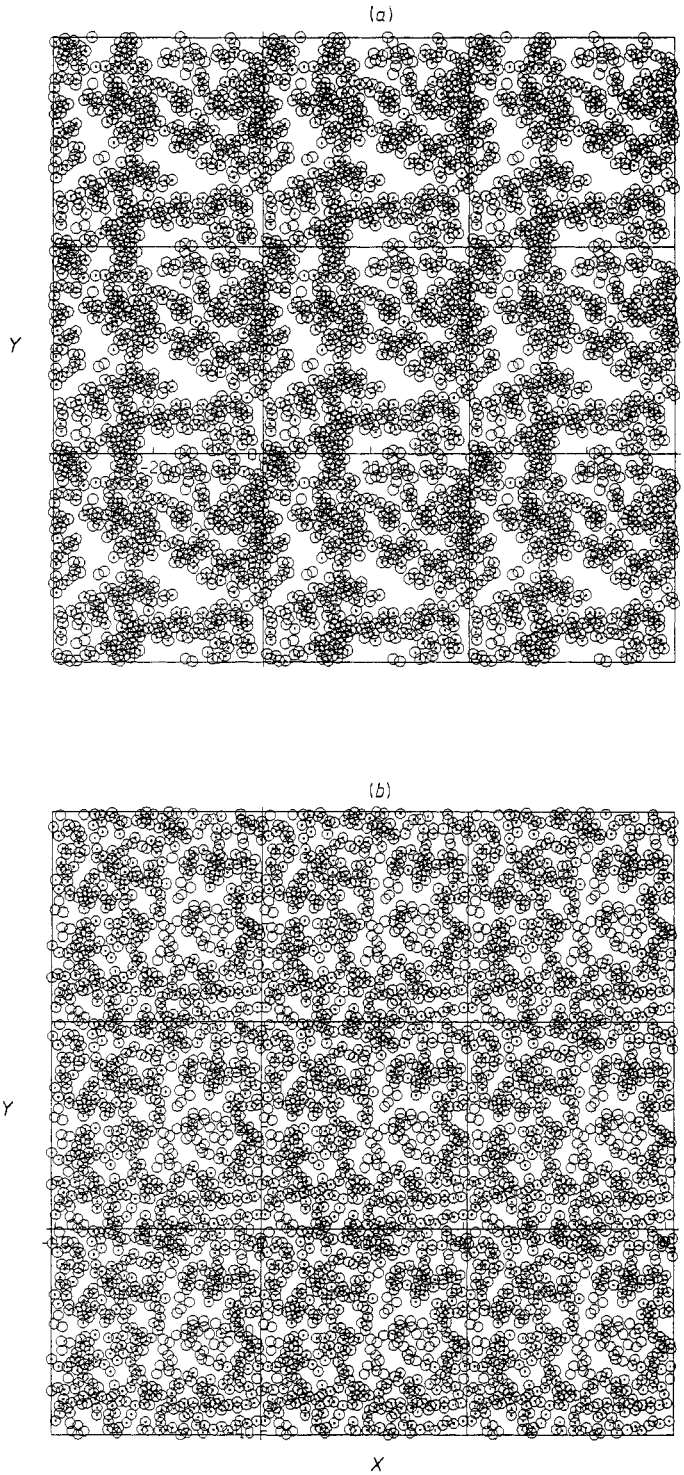

Figure 4. As for figure 2, except that $\sigma_s = 2.0$, $N = 450$ and the following states at p_c: (*a*) $T = 0.6, p = 0.307$; (*b*) $T = 5.0, p = 0.270$.

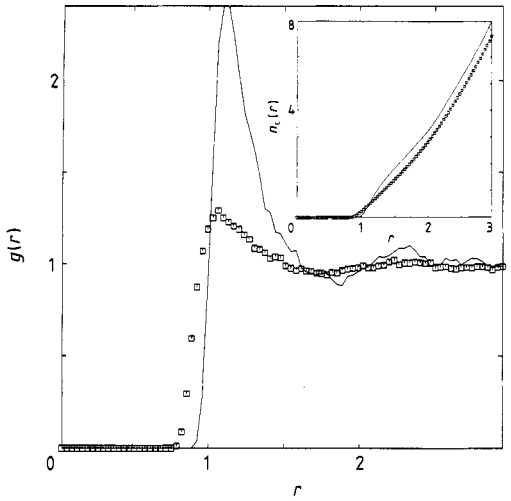

Figure 5. As for figure 3, except that $p = 0.265$.

Although the percolation threshold is a statistically well-defined state point for chosen T and σ_s, the percolating clusters change in appearance very rapidly. This is seen in figure 9 for the state point $T = 5.0$, $\rho = 0.4459$ and $\sigma_s = 1.5$. The two configurations shown in the figure are at intervals of 1 LJ time unit. (This corresponds to 2 ps for LJ argon.) They are very different in appearance. It leads one to question whether in a *molecular* system the percolating clusters *themselves* can have any significance for dynamical properties. There are short-range geometrical changes associated with the

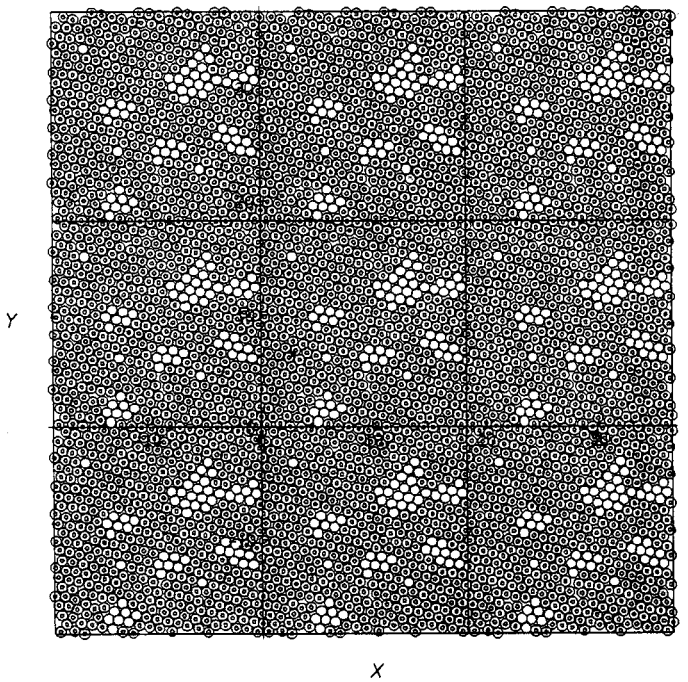

Figure 6. As for figure 2, except a hard-core state is chosen, $\sigma_s = 0.9$, $T = 10.0$ and $p = 1.345$.

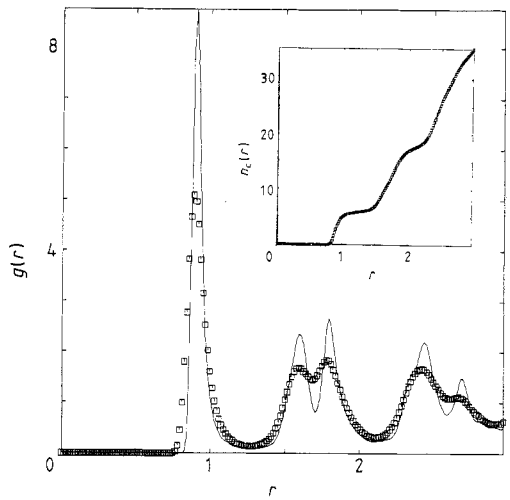

Figure 7. As for figure 3, except that $p = 1.33$.

percolation threshold (Heyes and Melrose 1989) which could change the density and temperature dependence of the transport coefficients at the percolation threshold. In figure 10 we show how the PC varies with time for the hard-core state, $T = 0.6$, $\rho = 1.1073$ and $\sigma_s = 1.0$. There the PC changes with time in a striking manner. At this low temperature the percolating and non-percolating particles partition themselves into zones on a triangular lattice. In the fluid phase, close to the solid coexistence line, i.e., with $\sigma_s \sim 1.2$, the PC become more tenuous with increasing temperature.

Approximately, ~70% of the molecules take part in the PC for $N = 450$ and 1250, rising to ~80% for $N = 50$. The maximum size of the non-percolating cluster is about $0.4\,N$, occurring at a density just below p_c.

The coordination number, that is the average number of neighbours within σ_s, decreases as temperature increases above T_c. For example, at $T = 10$ and $\sigma_s = 1.0$ the coordination number is 2.1 taking all neighbours whereas it is 2.3 for particles only within the percolating cluster. At $T = 0.75$ these numbers are 2.2 and 2.4, respectively. In the soft-core limit this trend is more pronounced. At $T = 10$ and $\sigma_s = 1.75$ the coordination number is 2.7 considering all particles and 2.9 taking particles only within the PC. At $T = 0.75$ these quantities have risen to 3.2 and 3.3 respectively. These trends are consistent with extra agglomeration of LJ particles as the temperature drops at low density.

We now consider the percolation exponents. There is evidence that the percolation exponent on lattices, random lattices and random continuum systems are the same or 'universal' (Kim *et al* 1987, Gawlinski and Stanley 1981). When compared with previous lattice percolation studies these continuum systems contain a much smaller number of particles to form clusters, compared with occupied sites in an equivalent lattice. We are confined to smaller cluster sizes before finite-N artefacts dominate. Therefore comparatively larger uncertainties exist on the exponents. *Based on a small s resolution*, deviations from 2D universality appear in at least one of the exponents of the 2D LJ fluids.

The cluster number distribution function, $n_s(s)$ has the exponent, $\tau = 2.05$ on a lattice randomly occupied (Stauffer 1979). We have obtained τ from log–log plots of $n_s(s)$ against s. Also, using a bin size that increases exponentially with s, we have adjusted τ to obtain a plateau in $n_s(s)/s^{-\tau}$. Both methods yield the same value of τ within the statistical uncertainty of the simulation data. We find that τ decreases from 2.0 ± 0.05

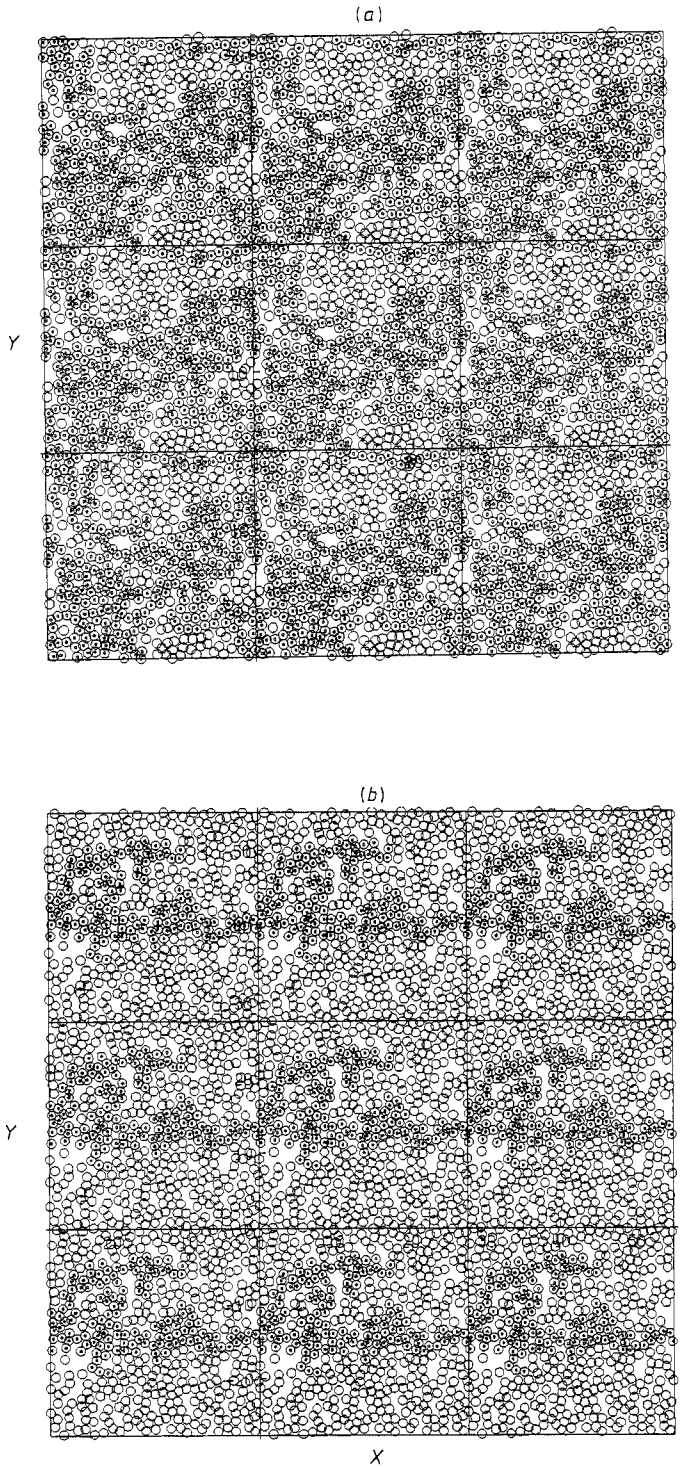

Figure 8. Pictoral illustration of non-percolating and percolating clusters in two-dimensional periodically repeating cells at a distance from the percolation threshold taken from 2D LJ MD simulations with $\sigma_s = 1.2$: (*a*) $\varepsilon = 0.0045$, $T = 10.0$; (*b*) $\varepsilon = 0.10$, $T = 10.0$. $N = 450$.

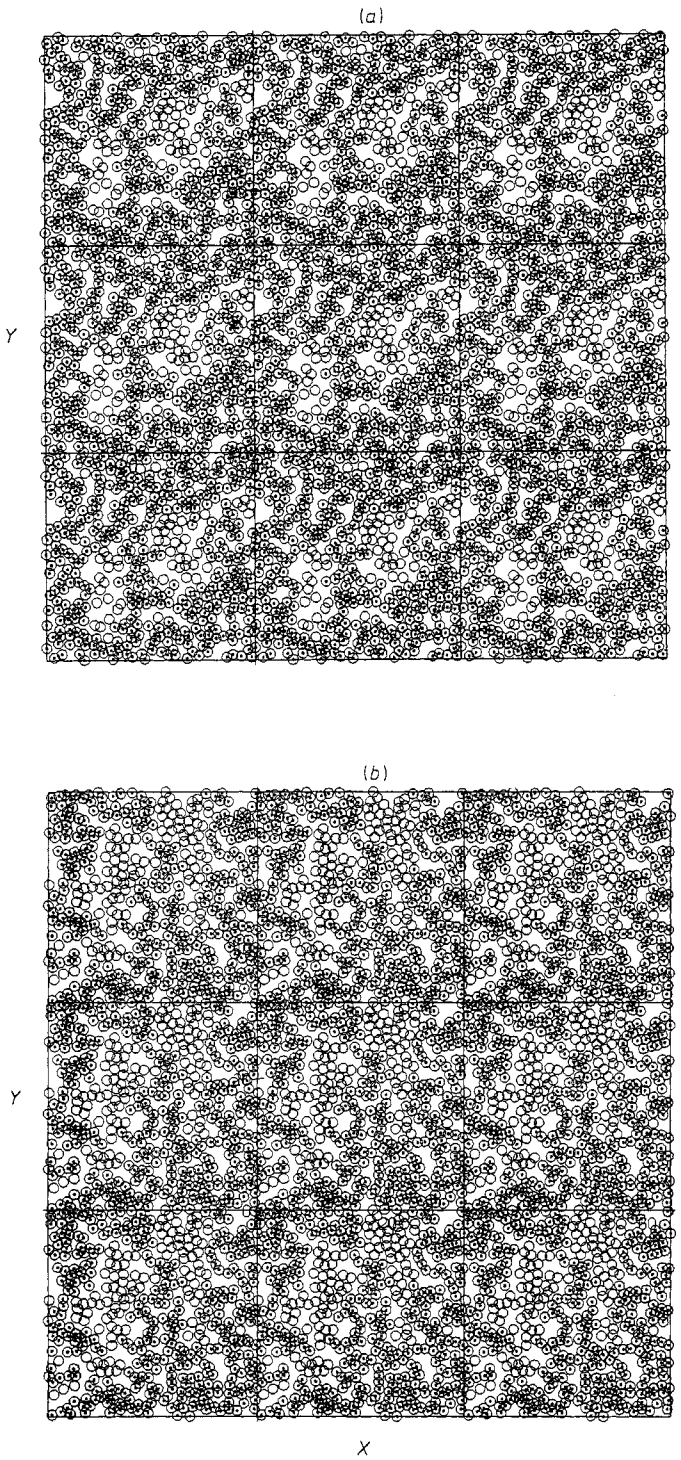

Figure 9. Pictoral illustration of the time-dependence of the non-percolating and percolating clusters at the percolation threshold. $\sigma_s = 1.5$, $N = 450$, $p = 0.446$ and $T = 2.0$. If the time since the start of the production simulation is t then, (*a*) $t = 2.0$ and (*b*) $t = 3.0$.

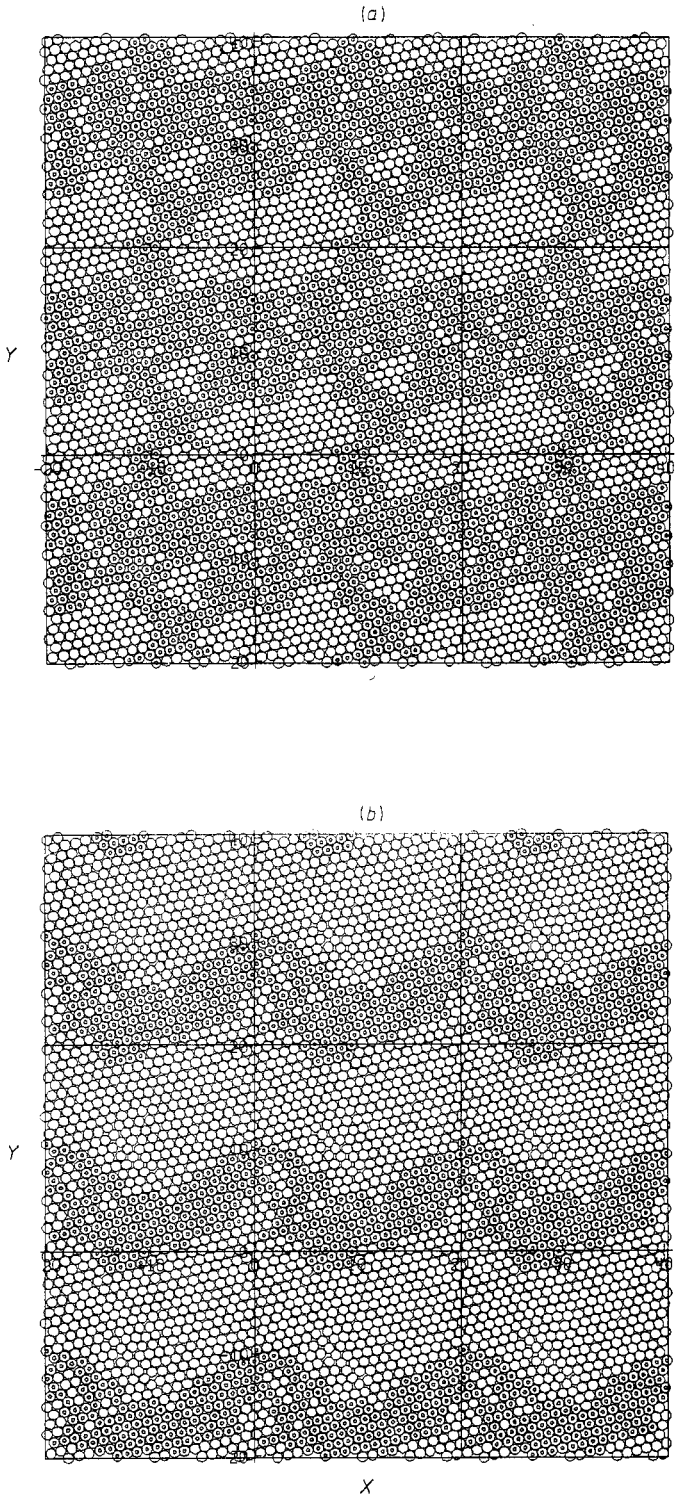

Figure 10. As for figure 9, except that $\sigma_s = 1.0$ and $p = 1.107$: (*a*) $t = 2.1$, (*b*) $t = 3.3$.

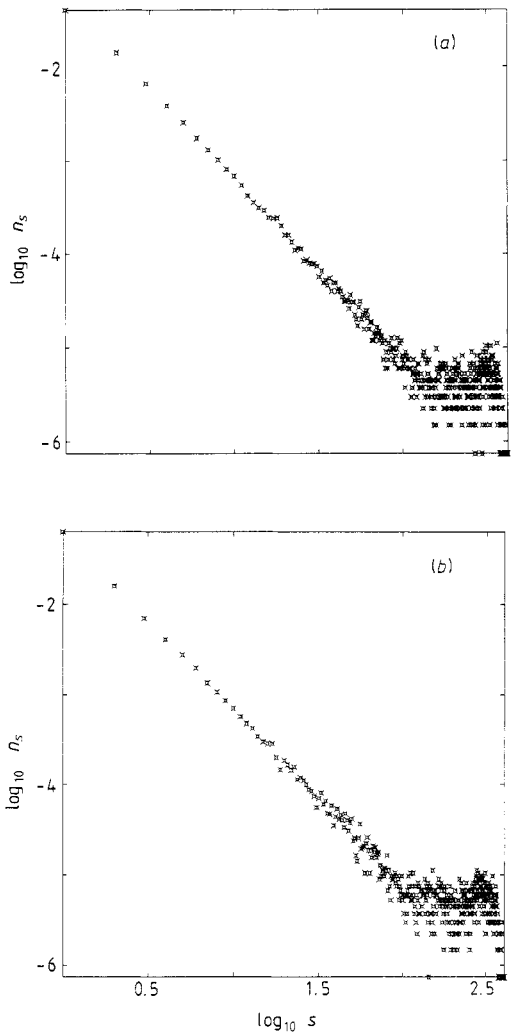

Figure 11. The cluster number distribution for non-percolating clusters, $n_s(s)$ for the LJ ($N = 450$) LJ state points at p_c: (*a*) $T = 10.0$, $p = 1.345$, $\sigma_s = 0.9, \tau = 1.91 \pm 0.05$; (*b*) $T = 1.0, p = 0.832$, $\sigma_s = 1.1, \tau = 1.97 \pm 0.05$.

in the (high-density) hard-core limit to a value of 1.6 ± 0.1 in the (low-density) soft-core limit. Examples of n_s at p_c that demonstrate this trend are given in figure 11. Finite size effects distort $n_s(s)$ from the power law decay as $s \rightarrow$ N. We observe a similar trend in 3D LJ going from $\tau = 2.0 \pm 0.05 \rightarrow 1.85 \pm 0.05$. (In 3D the universal value for τ is 2.2 for randomly occupied lattices (Stauffer 1984).)

The non-percolating and percolating clusters formed from non-interacting particles on a lattice at p_c manifest the same fractal dimension, D_f. For non-interacting particles, percolation theory gives $D_f = D - \beta/\nu$, where D is the dimension of the space (= 2 here) and β and ν are the percolation exponents. In 2D, $\beta = 0.14$ and $\nu = 1.35$ (Stauffer 1979). Therefore $D_f = 1.90$. As for τ we obtained D_f by two routes from the radius of gyration of the non-percolating clusters. A log–log plot of R_g against s has a slope of $1/D_f$, illustrated in figure 12. Also, using a bin size that increases exponentially with s, we have adjusted D_f to obtain a plateau in $R_g(s)/s^{1/D_f}$. Both methods yield the same value of D_f.

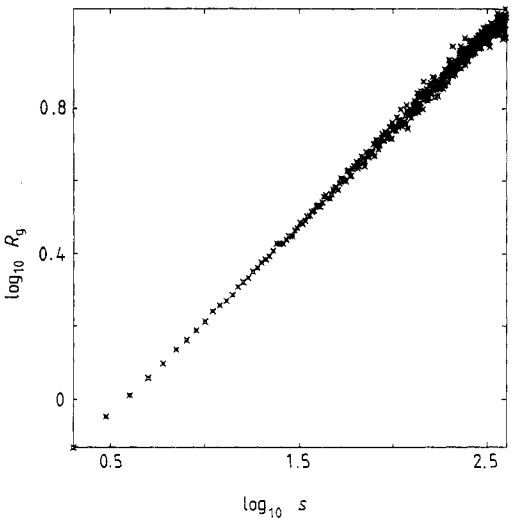

Figure 12. The s-dependence of the radius of gyration R_g for the $N = 450$ LJ state points at the percolation threshold with $T = 1.0, p = 0.832$ and $\sigma_s = 1.1$, $D_f = 1.04 \pm 0.05$. We used $R_g \propto s^{1/D_f}$.

Although, the statistics degenerate in the soft-core limit, we find that D_f is 1.9 ± 0.1 independent of temperature from the hard-core extreme to the soft-core limit.

The pair connectivity function gives D_f of the percolating cluster(s) at p_c. At intermediate distances, in terms of the simulation cell sidelength, $p(r) \propto r^{D_f - 2}$. Therefore D_f could be extracted from a log–log plot of $p(r)$ against r. In practice, this part of $p(r)$ is partially obscured by the short-range structure. An example of $p(r)$ and $g(r)$ are given in figure 13. The number of particles contained within radius r about a particle varies as r^{D_f} as $r \rightarrow \infty$. This function, obtained by integrating $p(r)$, gives statistically better values for D_f for the *percolating* cluster. At p_c the D_f from R_g and $p(r)$ are statistically indistinguishable.

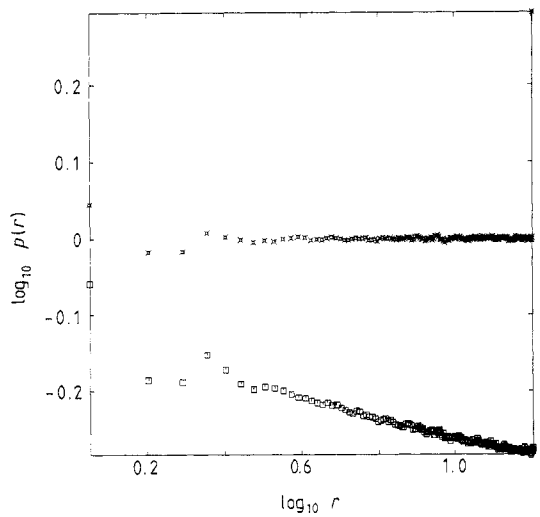

Figure 13. Log–log plot of $g(r)$ (×), and $p(r)$ (□) at the percolation threshold. $N = 450, p = 0.441$, $T = 10.0$, $\sigma_s = 1.5$ and $D_f = 1.84 \pm 0.05$.

5. Conclusions

We have demonstrated that the percolation cluster statistics of the two-dimensional, Lennard-Jones fluid and solid can be interpreted directly from changes in the short range structure measured by the pair radial distribution function. In molecular fluids the shape of the percolating cluster changes markedly on the timescale of a molecular vibration. Martin *et al* (1987) showed that mobile (attractive) interacting particles on a lattice probably belong to the same universality class as those of non-interacting lattice particles (i.e., have the same exponents). We present evidence that suggests there may be departures from this in the soft-core limit for continuum interacting systems. Although this is tentative until molecular dynamics simulation is capable of treating much larger samples, comparable with those considered in 2D lattice models, e.g. $\sim 10^{10}$ sites (Stauffer 1984, 1986). Crossover effects occurring at larger cluster size than treated here cannot be ruled out.

Acknowledgments

DMH gratefully thanks The Royal Society for the award of a Royal Society 1983 University Research Fellowship. JRM thanks SERC and MOD for the award of a post-doctoral research fellowship. We acknowledge with gratitude the SERC for the award of computer time on the CRAY-1S at the University of London Computer Centre, and the Royal Holloway and New Bedford College Computer Centre for use of their computing facilities. We thank a referee for helpful suggestions on refining the values of the exponents.

References

Balberg I 1988 *Phys. Rev.* B **37** 2391
Balberg I and Binenbaum N 1987 *Phys. Rev.* A **35** 5174
Bug A L R, Safran S A, Grest G S and Webman I 1985 *Phys. Rev. Lett.* **55** 1896
Gawlinski E T and Stanley H E 1981 *J. Phys. A: Math. Gen.* **14** L291
Herrmann H J 1986 *Phys. Rep.* **136** 153
Heyes D M 1987 *J. Chem. Soc. Faraday Trans.* II **83** 1985
Heyes D M and Melrose J R 1988 *J. Phys. A: Math. Gen.* **21** 4075
—— 1989 *Mol. Sim.* **2** 281
Kim D Y, Herrmann H J and Landau D P 1987 *Phys. Rev.* B **35** 3661
Martin H O, Albano E V and Maltz A L 1987 *J. Phys. A: Math. Gen.* **20** 1531
Reddy M R and O'Shea S F 1985 *Can. J. Phys.* **64** 677
Seaton N A and Glandt E D 11987 *J. Chem. Phys.* **86** 4668
Stauffer D 1979 *Phys. Rep.* **54** 1
—— 1984 *Introduction to Percolation Theory* (Chichester: Taylor and Francis)
—— 1986 *On Growth and Form* ed. H E Stanley and N Ostwesky (Amsterdam: Martinus Nijhoff) p 79